Enumeration method for the hole line expansion diagrams

R. Sartor

University of Liège, Institute of Physics B5, 4000 Liège 1, Belgium

We point out that to any order of the hole line expansion simple graph theoretical arguments yield an upper bound on the number of hole lines contained in the diagrams. The derivation of this upper bound suggests a procedure which could be useful in the actual enumeration of the hole line expansion diagrams. The cases of the binding energy and of the mass operator are treated in sufficient detail to make obvious the extension of our results to other quantities. [S0556-2813(97)00408-1]

PACS number(s): 24.10.Cn, 21.10.Dr, 21.60.−n, 21.65.+f

I. INTRODUCTION

The hole line expansion constitutes one of the widely accepted methods (see, e.g., [1]) used in the study of nuclear matter. As is well known, it results from ordinary perturbation theory by performing two diagram rearrangements. The first one consists in summing the so-called particle-particle ladders into the Brueckner reaction matrix G: this solves the problems raised by the short-range behavior of the nucleon-nucleon force. The second rearrangement consists in ordering the diagrams according to the number of independent hole line momenta, i.e., the hole momenta which remain after momentum conservation has been taken into account. The ensuing expansion then appears to be ruled by the small parameter κ which measures the ratio of the two-body correlation volume to the mean volume occupied by a nucleon. Hole line momentum independence appears to be crucial to partition the whole set of diagrams into classes of diagrams of given order in κ. For instance, the so-called hole-hole diagram which involves four hole lines (see Fig. 1) should be considered on the same footing as the three-body cluster diagrams of Fig. 2 which only involve three hole lines: estimates indeed show that all these diagrams are reduced by a single factor κ with respect to the leading Brueckner-Hartree-Fock (BHF) contribution. Many other examples of this ordering rule can be found, e.g., in [2] where the class of binding energy diagrams with four independent hole lines is studied.

This leads us to inquire whether there is an upper bound on the number h of holes lines in diagrams of order I, i.e., in diagrams with I independent hole lines. This question will be answered in the affirmative: to any order I is associated an upper bound on the number h of hole lines which can appear in the diagrams contributing to that order. A related question concerns the actual enumeration of the diagrams of order I with $h>I$: can we find some simplification which could enable us to avoid examining all the diagrams with h hole lines to see whether or not momentum conservation will reduce the h hole lines to I-independent ones? The answer to this question is again in the affirmative. We shall show that the diagrams of order I with $h>I$ hole lines can all be constructed by assembling a well defined number of subdiagrams belonging to classes whose enumeration is much easier than the enumeration of the complete class of diagrams with h hole lines. This stems from the fact that all the subdiagrams referred to above have less than I hole lines.

This paper is organized as follows. In Sec. II, we study the binding energy and the mass operator and we derive the corresponding upper bounds on the number h of hole lines allowed at any order I of the hole line expansion. In Sec. III, we analyze the structure of diagrams as a function of h and I. This analysis suggests a simplified enumeration procedure which we apply in Sec. IV to the detailed study of an ex-
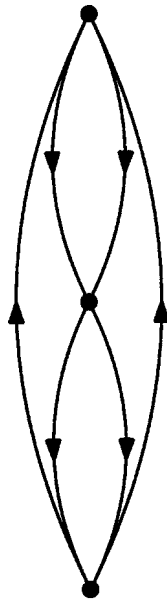

FIG. 1. The so-called hole-hole contribution to the binding energy of nuclear matter. Here as well as in the other figures of this paper, full dots represent antisymmetrized G matrices.
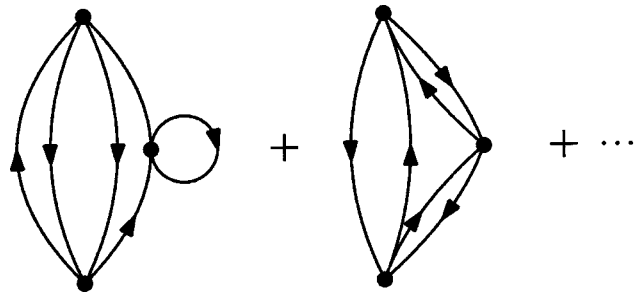

FIG. 2. Diagrams pertaining to the three-body-cluster contribution to the binding energy of nuclear matter.

ample. Our work is summarized and compared with related ones in Sec. V.

II. HOLE LINE NUMBER UPPER BOUNDS AT ANY ORDER OF THE HOLE LINE EXPANSION

A. Binding energy diagrams

Because of momentum conservation, the momenta attached to the hole and particle lines of any diagram D can all be expressed in terms of a subset of them; namely, the subset of the so-called independent momenta. These are the momenta which are integrated over in the analytical expression corresponding to the given diagram. Such a subset of independent momenta can be obtained by considering any spanning tree T contained in D. (We remind the reader that by definition, a tree is a connected loop free diagram and that a tree T is said to span a diagram D when it has the same vertices as D, whereas its line set is a subset of the line set of D.) The looked for independent momenta are then the momenta attached to the lines which do not belong to T. Hence, to determine the number I of independent hole momenta in D, one has to find a spanning tree which contains as few hole lines as possible. Henceforth, such a tree will be called a minimal spanning tree. It can be constructed by means of the following method. First we suppress all the hole lines of D. In general, this will yield a disconnected diagram with, say, N connected components. Then we construct a spanning tree for each component; this yields a collection of subtrees which only involve particle lines. Finally, we link these subtrees into a spanning tree by using $N-1$ of the previously suppressed hole lines. It should be clear that this spanning tree is minimal. Indeed the connected components referred to above exist independently of our construction method and any spanning tree will have to use up exactly $N-1$ hole lines between these components in order to link them together. It should also be clear that in any spanning tree which is not minimal, the extra hole lines will never be hole lines between components since using more than $N-1$ such lines would create loops which by definition are not allowed in a tree: any extra hole line has to link vertices belonging to the same component. In the following, a component together with the hole lines between its vertices will be referred to as a subdiagram. In Fig. 3, the method we have just described is illustrated on the hole-hole diagram of Fig. 1.

Our results so far can be summarized for any diagram D by the equation

$$I=h-N+1, \tag{2.1}$$

where h is the total number of hole lines in D and I is the number of independent ones, i.e., the order of D within the framework of the hole line expansion. N is as above the number of components or subdiagrams determined by the method we used to construct the minimal spanning tree.

Now, we want to prove that for any binding energy diagram, we have

$$h \geqslant 2N. \tag{2.2}$$

The proof is trivial when $N=1$. Indeed either the considered diagram is the BHF one (see Fig. 4) for which we have $h=2$ or its lowermost vertex is a vertex of type A (see Fig. 5)
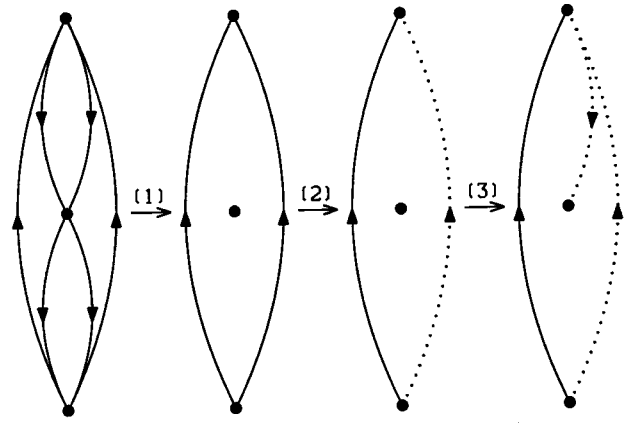

FIG. 3. Determination of the minimal spanning tree on an example. Step (1): Suppress the diagram hole lines. This leads to a diagram with $N=2$ components. Step (2): Construct a spanning tree for each component. In this example, one of the components consists of a single vertex and the corresponding tree is reduced to that vertex. The other component consists of two vertices linked by two particle lines. One possible tree is indicated by the dotted line. Step (3): Link the trees obtained in the previous step to form a minimal spanning tree (dotted lines).

which already involves two hole lines. Hence in both cases, the inequality (2.2) is obviously satisfied. In order to treat the $N>1$ case, we shall use the graph theory theorem which states that if we define the degree of a vertex as the number of lines which are attached to it, then the sum of the degrees of all the vertices in a diagram is equal to twice the number of lines. The proof of this theorem just consists in noticing that since a line is necessarily attached to two vertices (distinct or not), it will be counted twice when we calculate the sum of the degrees by mere counting and adding. This simple proof suggests an interpretation of the theorem by stating that each line in the diagram contributes half a unit to the total count of lines when ''seen'' from any of the two vertices (distinct or not) that it links together. This interpretation will be used several times in the following.

Consider now the collection of vertices $(A, \ldots, M)$ from which any diagram is constructed (see Fig. 5). One notices that the difference d between the number of hole and particle lines above any vertex is always the same as below it (for instance, we have $d=0$ for the vertices A, B, and H). This implies that each of the N subdiagrams which appear in the minimal tree construction, is linked to the other ones by an even number of hole lines, half of them incoming and the other half outgoing (see Fig. 6). Moreover, since we only consider connected diagrams each subdiagram has to be linked to the rest of the diagram by at least two hole lines. In the following, we shall refer to the hole lines inside a subdiagram as its internal hole lines and to the hole lines which
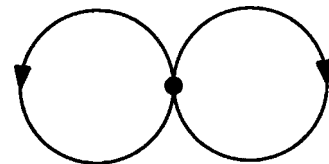

FIG. 4. Brueckner-Hartree-Fock (BHF) contribution to the binding energy of nuclear matter.
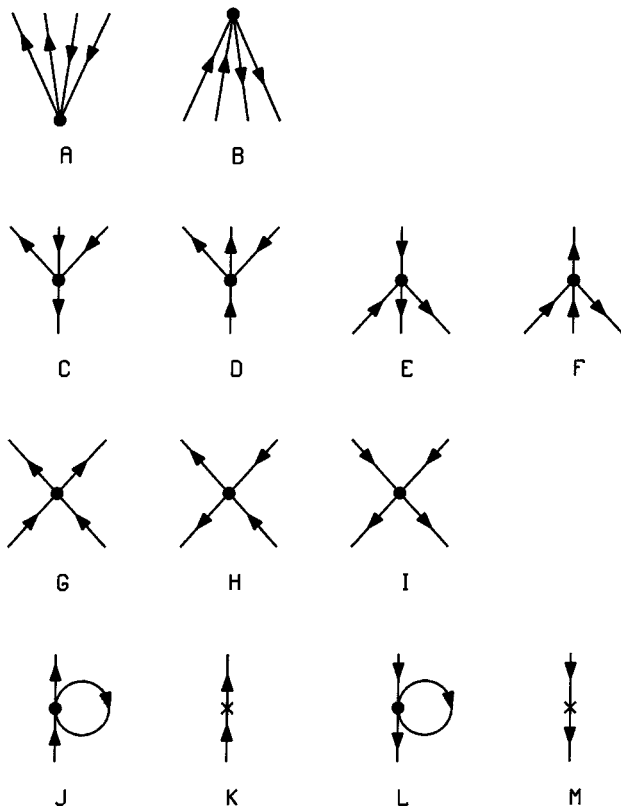
FIG. 5. List of possible vertices. Crosses refer to auxiliary potential (U) insertions. Note that it is convenient to consider the "tadpoles" J and L as vertices when constructing the diagrams.

link it to the rest of the diagram as its external hole lines. Consider now a given subdiagram s and denote by h_i and h_e the numbers of its internal and external hole lines, respectively. The contribution h_s of s to the total number h of hole lines in the diagram will be given by

$$h_s = h_i + \frac{h_e}{2}, \quad (2.3)$$

where the factor $\frac{1}{2}$ multiplying h_e is derived from the interpretation we have given of the above mentioned theorem when applied to an auxiliary diagram obtained from the diagram under scrutiny by shrinking the subdiagrams to points while keeping the set of external hole lines.
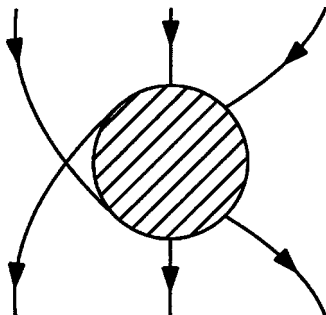

FIG. 6. Subdiagram structure: Any subdiagram is linked to the rest of the diagram by an even number of hole lines, half of them incoming and the other half outgoing.
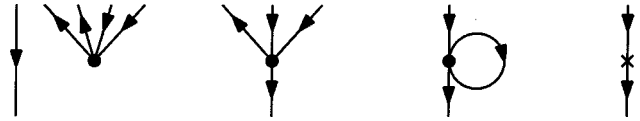

FIG. 7. List of the possible lowermost vertices for subdiagrams with two external hole lines.

Hence, for subdiagrams with at least four external hole lines we obtain (without having to discuss the allowed values of h_i)

$$h_s \geq 2. \quad (2.4)$$

On the other hand, we have to show that h_i cannot vanish if we want to write an inequality identical to Eq. (2.4) for the subdiagrams with two external hole lines. This can be seen from Fig. 7 where we have depicted all the possible lowermost vertices for a subdiagram with two external hole lines. In all cases, the lowermost vertex involves an internal hole line (we assume that the auxiliary potential appearing in the fourth diagram of Fig. 7 is self-consistent at least at the BHF level which implies a "hidden" hole line).

Hence Eq. (2.4) applies to any subdiagram and by summing over the contributions h_s of all subdiagrams we obtain the inequality (2.2). By combining Eq. (2.1) with Eq. (2.2), we obtain

$$h \leq 2I - 2, \quad (2.5)$$

which gives the upper bound on the number h of hole lines allowed at any order I of the hole line expansion. Note that this upper bound cannot be improved since for any order I, one can find diagrams with $h = 2I - 2$ hole lines. Figure 1 provides an example for $I = 3$ and it should be obvious that one can construct similar diagrams for any I.

B. Mass operator diagrams

We now consider the mass operator whose hole line expansion has been advocated and discussed in [3]. To construct the minimal spanning tree, one proceeds as for the binding energy diagrams. A minor difference only appears in the first step of the procedure: here one has to suppress not only the hole lines of the diagram but also the so-called legs whose momenta are in fact given momenta. Then, Eq. (2.1) also applies here with the same meaning for the symbols I, h, and N.

Now, we want to show that Eq. (2.2) has to be replaced by

$$h \geq 2N - 1. \quad (2.6)$$

In order to prove this, we have to consider two cases. In the first one, both legs of the diagram are attached to the same subdiagram (a subdiagram is defined as in Sec. II A). Since these legs have replaced two external hole lines, the contribution h_s of this subdiagram to the total number of hole lines will be reduced by one unit and will satisfy the inequality

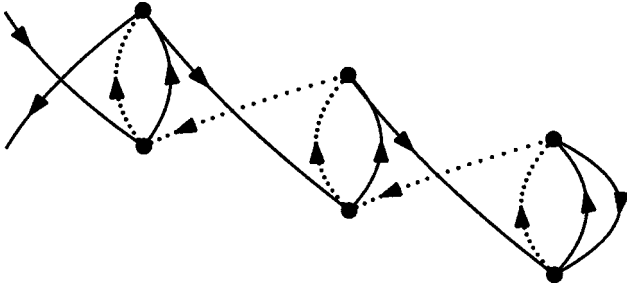$$h_s = h_i + \frac{h_e}{2} \geq 1. \quad (2.7)$$

FIG. 8. Example of a diagram corresponding to the upper bound $h = 2I - 1$ in Eq. (2.11). The dotted lines define a minimal spanning tree.

For the other subdiagrams the inequality (2.4) will still apply. By summing the contributions h_s of all subdiagrams, we obtain

$$h = \Sigma h_s \geq 1 + 2(N-1) \geq 2N - 1, \qquad (2.8)$$

i.e., the inequality (2.6). In the second case to be considered, the diagram legs are attached to two distinct subdiagrams. Since in each of these subdiagram a leg has replaced an external hole line, the contribution h_s of each of them to the total number of hole lines will be reduced by half a unit and will satisfy the inequality

$$h_s = h_i + \frac{h_e}{2} \geq \frac{3}{2}. \qquad (2.9)$$

Again, inequality (2.4) will apply to the other subdiagrams. By summing the contributions h_s of all the subdiagrams, we obtain

$$h = \Sigma h_s \geq 2\left(\frac{3}{2}\right) + 2(N-2) \geq 2N - 1, \qquad (2.10)$$

i.e., the inequality (2.6).

By combining Eqs. (2.1) and (2.6), we obtain

$$h \leq 2I - 1, \qquad (2.11)$$

which provides the upper bound on h at any order I of the hole line expansion pertaining to the mass operator. Note that this upper bound cannot be improved since at any order I, one can construct diagrams which satisfy $h = 2I - 1$. An example of such a diagram is provided in Fig. 8.

III. STRUCTURE OF THE HOLE LINE EXPANSION DIAGRAMS

The inequalities (2.5) and (2.11) show that the number h of hole lines allowed in diagrams increases almost twice as fast as the order I which has been retained in the hole line expansion. This implies that except at the lowest order, where $h = I$ for both the binding energy and the mass operator, one will have to perform the time consuming enumeration of lots of diagrams with $h > I$ just to check whether or not momentum conservation reduces the number of hole integrations down to I. Our aim will be to show that the subdiagram structure we have used in the discussion of Sec. II, can lead to a sizeable reduction of the enumeration work.

From Eq. (2.1) we see that $h > I$ implies $N > 1$, i.e., that the corresponding diagram can be seen as an assembly of subdiagrams linked together by external hole lines only. This suggests that we should enumerate the subdiagrams first and then assemble them into diagrams. This method reduces the enumeration task for the following reasons.

First, let us consider the subdiagrams pertaining to the binding energy. All of them have at least two external hole lines and we have seen in Sec. II that each external hole line contributes half a unit to the total number h of hole lines in the diagram. This means that together the external hole lines of the N subdiagrams will contribute at least N units to h. From Eq. (2.1) we then see that at most $I - 1$ internal hole lines will remain shared among the N subdiagrams. Hence, for all the $h > I$ values allowed by the upper bound (2.5) we just have to enumerate the subdiagrams with at most $I - 1$ internal hole lines. Actually there is a stronger limit on the number of internal hole lines allowed in subdiagrams with more than $I - 1$ external hole lines. Indeed, for any subdiagram one has trivially

$$h_i + h_e \leq h, \qquad (3.1)$$

which together with Eq. (2.5) yields

$$h_i \leq 2I - 2 - h_e. \qquad (3.2)$$

When h_e is (strictly) bigger than $I - 1$, the right-hand side of this inequality yields an upper bound on h_i which is indeed lower than $I - 1$. One should note that there is also an upper bound on the number of external hole lines attached to any subdiagram. Indeed, Eqs. (2.5) and (3.1) also imply

$$h_e \leq 2I - 2. \qquad (3.3)$$

Finally, the number N of subdiagrams which can appear in any diagram is also bounded at each order I of the hole line expansion. This can be seen from the inequalities (2.2) and (2.5), which together yield

$$N \leq I - 1. \qquad (3.4)$$

Let us now consider the mass operator diagrams. Here too, the enumeration of subdiagrams followed by their assembly is easier than the direct enumeration of all the diagrams satisfying the inequality (2.11). Let us first establish the upper bound on the number h_i of internal hole lines. In the case of a mass operator diagram, the contribution of the external hole lines to the total number of hole lines can be as low as $N - 1$ (instead of N for binding energy diagrams) since the diagram legs have replaced two external hole lines. From Eq. (2.1), we conclude that at most I internal hole lines remain to be shared by the subdiagrams. This means that we can limit ourselves to the enumeration of subdiagrams with at most I internal hole lines for all h values allowed by the inequality (2.11). By combining Eq. (2.11) with Eq. (3.1), one gets

$$h_i \leq 2I - 1 - h_e, \qquad (3.5)$$

whose right-hand side yields a stronger upper bound on h_i for subdiagrams with more than $I - 1$ external hole lines.

From Eqs. (2.11) and (3.1), one also derives the following upper bound on the number of external hole lines which can be attached to a subdiagram:

$$h_e \leq 2I - 1. \qquad (3.6)$$

Finally, from Eqs. (2.6) and (2.11), one derives

$$N \leq I, \qquad (3.7)$$

which gives the upper bound on the number N of subdiagrams.

As will appear in the next section, the enumeration of subdiagrams in the mass operator case becomes easier if we do not worry for each subdiagram about which external hole lines could possibly act as the diagram legs: all mass operator subdiagrams will actually be drawn as binding energy subdiagrams, i.e., as if all their ''legs'' were external hole lines. The number h'_e of these undifferentiated external hole lines will always be even and it will exceed the number h_e of actual external hole lines by at most two units:

$$h'_e \leq h_e + 2. \qquad (3.8)$$

This together with Eq. (3.5) implies

$$h_i \leq 2I + 1 - h'_e, \qquad (3.9)$$

which improves on the upper bound I on h_i when h'_e is bigger than $I + 1$. Finally, the upper bound on h'_e is derived from Eqs. (3.6) and (3.8), which yield

$$h'_e \leq 2I + 1 \leq 2I, \qquad (3.10)$$

where the fact that h'_e is even has been taken into account to write the last inequality.

IV. ENUMERATION EXAMPLE

In this section, we shall enumerate the contributions to the mass operator up to two independent hole lines. We shall thus illustrate the results obtained above and point out some peculiar features in the construction of subdiagrams when two or more of them have to be assembled to yield a complete mass operator diagram.

The contributions to the mass operator with one independent hole line ($I = 1$) are readily obtained with the above method. Indeed, Eq. (2.11) implies that only diagrams with a single hole line ($h = 1$) will be involved and from Eq. (2.1) one sees that they will be obtained from a single subdiagram ($N = 1$), i.e., that no assembly will be required. From Eq. (3.10), we see that we just have to enumerate the subdiagrams with two undifferentiated external hole lines ($h'_e = 2$); these external hole lines will actually constitute the diagram legs. The subdiagrams satisfying all these requirements are depicted in Fig. 9 (for definiteness we assume that the auxiliary potential is self-consistent at the one hole line level). Diagram (a) is the well-known BHF contribution, whereas diagram (b) just serves to cancel a similar contribution coming from the unperturbed part of the mass operator. One should note that in keeping with the remarks at the end of Sec. III, we have drawn the mass operator legs as hole lines although this does not imply any constraint on the mo-
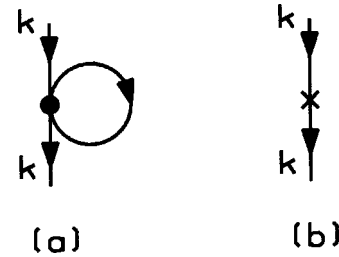

FIG. 9. One hole line contributions to the mass operator.

mentum $\mathbf{k}$ associated with these lines: $|\mathbf{k}|$ can be bigger as well as lower than the Fermi momentum.

Let us now consider the contributions with two independent hole lines ($I = 2$). From Eqs. (2.11) and (2.1), one derives that the values which are allowed for h and N are ($h = 2$, $N = 1$) and ($h = 3$, $N = 2$). Each diagram ($h = 2$, $N = 1$) consists of a single subdiagram. This rules out subdiagrams with $h'_e = 4$ which would be allowed by Eq. (3.10); hence, we just have to consider subdiagrams with two undifferentiated external hole lines ($h'_e = 2$). As in the $I = 1$ case, these hole lines will be the legs of the diagram. Let us note that when we build the subdiagrams from the vertices depicted in Fig. 5, we can disregard vertices I, L, and M. Indeed, these vertices are actually unallowed subdiagrams: vertex I corresponds to a subdiagram with $h'_e = 4$, whereas vertices L and M correspond to subdiagrams with $h = 1$. By combining the remaining vertices of Fig. 5, one can build the ($h = 2$, $N = 1$) diagrams shown in Fig. 10. Diagrams (a)–(e), which contain a box labeled G^n, stand for an infinite series of diagrams which are obtained by replacing the box by $n = 0, 1, 2, \ldots$, vertices of type G (refer to Fig. 5 for the various vertex types). As an example, the diagrams corresponding to Fig. 10(a) for $n = 0$, 1, and 2 are displayed in Fig. 11. Note that there is a single diagram for each n because in order to avoid double counting, successive G vertices should never be linked together by two particle lines. Diagrams (a)–(j) in Fig. 10 can all be obtained from the so-called three-body-cluster diagrams pertaining to the hole line expansion of the binding energy [4] by ''cutting'' a hole line. Diagram (k) can also be obtained from a binding energy diagram by cutting a hole line. In contradistinction diagram (l) does not correspond to any binding energy diagram since by ''pasting together'' the diagram legs one would obtain a diagram with two successive G matrices linked by two particle lines. Note, however, that such diagrams are not forbidden when one writes the binding energy as the sum of the true kinetic and potential energies (see [5]).

We now consider the ($h = 3$, $N = 2$) diagrams, i.e., the diagrams composed of two subdiagrams. First, we enumerate these subdiagrams. From Eq. (3.10) with $I = 2$, one concludes that only subdiagrams with $h'_e = 2$ or 4 are allowed. For subdiagrams with $h'_e = 2$, the number of internal hole lines cannot vanish [see discussion following Eq. (2.4)] so that one can have $h_i = 1$ or 2. For subdiagrams with $h'_e = 4$, the improved upper bound on h_i given by Eq. (3.9) applies and only the values $h_i = 0$ or 1 are allowed. Thus, we have to find the subdiagrams characterized by $(h'_e, h_i) = (2, 1)$, (2, 2), (4, 0), and (4, 1). The search can be simplified a little further by noticing that for any diagram composed of at least
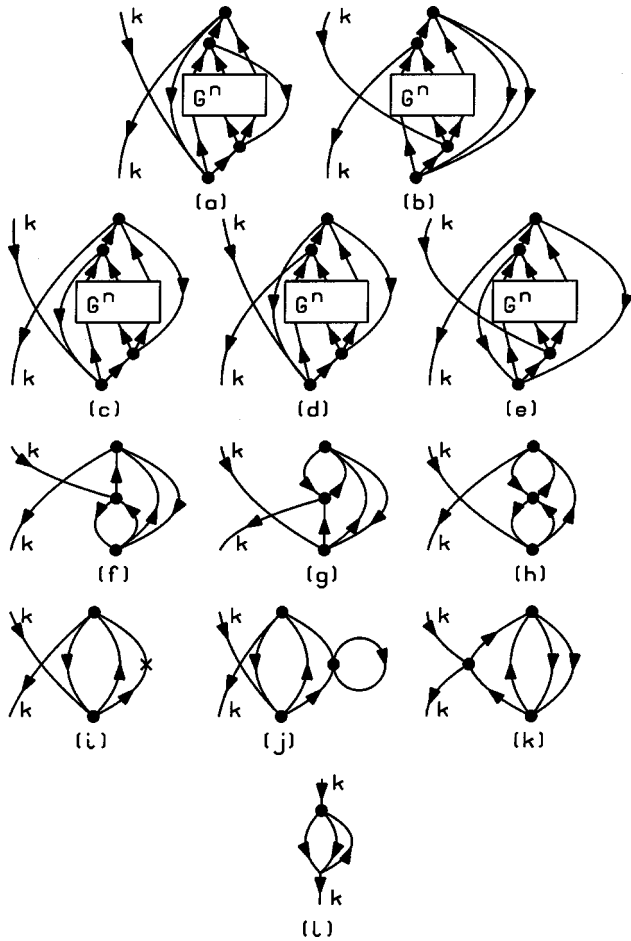
FIG. 10. Two hole line contributions to the mass operator consisting of a single subdiagram.
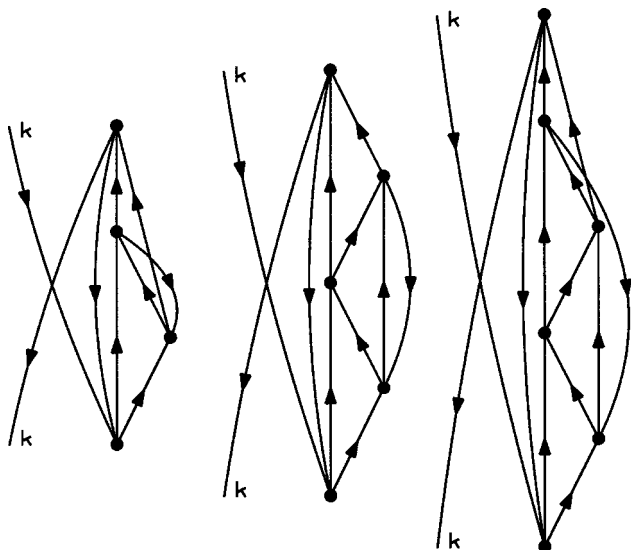

FIG. 11. Diagrams obtained from Fig. 10(a) when the box labeled G^n is replaced by n G matrices. The illustrated cases correspond to $n=0$, 1, and 2.
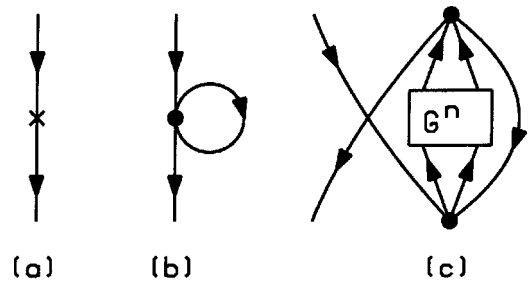

FIG. 12. Subdiagrams with two undifferentiated external hole lines and a single internal hole line. These subdiagrams are referred to as (2, 1) subdiagrams in the text.

two subdiagrams, one has

$$\frac{(\Sigma h_e')-2}{2}+(\Sigma h_i)=h. \tag{4.1}$$

This implies that ($h=3$, $N=2$) diagrams can only be constructed by using the following (h_e', h_i) combinations of subdiagrams: (2, 1)+(2, 1), (2, 1)+(4, 0), and (4, 0)+(4, 0). Actually, the combination (2, 1)+(2, 1) is ruled out by the fact that the diagram has to be one line irreducible to qualify as a mass operator diagram. Hence only the combinations (2, 1)+(4, 0) and (4, 0)+(4, 0) will have to be considered in the assembly process.

The allowed (2, 1) and (4, 0) subdiagrams are depicted in Figs. 12 and 13, respectively. The boxes labeled G^n have the same meaning as in Fig. 10. Let us stress that when constructing subdiagrams, one does not have to apply the rule stating that successive G matrices should never be linked by two particle lines. This rule only applies to the diagrams one constructs by assembling the subdiagrams. It will appear clearly below that by suitably ''interlocking'' subdiagrams containing such G-matrix ladders, one can always avoid double counting. Let us note in passing that all the diagrams summarized by Figs. 12(c) and 13(b) actually consist of G-matrix ladders.

Let us now assemble (2, 1) and (4, 0) subdiagrams to construct complete diagrams. The subdiagrams in Figs. 12(a) and 12(b) can only be assembled with the $n=0$ version of the subdiagram in Fig. 13(b). This yields the diagrams in Figs. 14(a) and 14(b). Similarly, the subdiagram in Fig. 13(a) can only be assembled with the $n=0$ version of the subdiagram in Fig. 12(c). This yields the diagram in Fig. 14(c). The $n=0$ version of the subdiagram in Fig. 12(c) can be com-
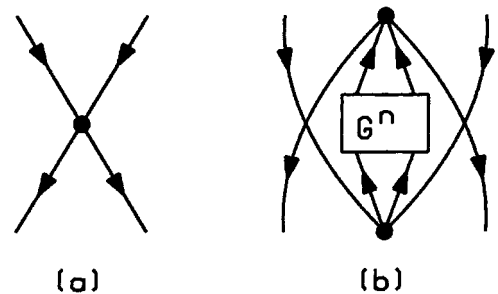

FIG. 13. Subdiagrams with four undifferentiated external hole lines and no internal hole line. These subdiagrams are referred to as (4, 0) subdiagrams in the text.
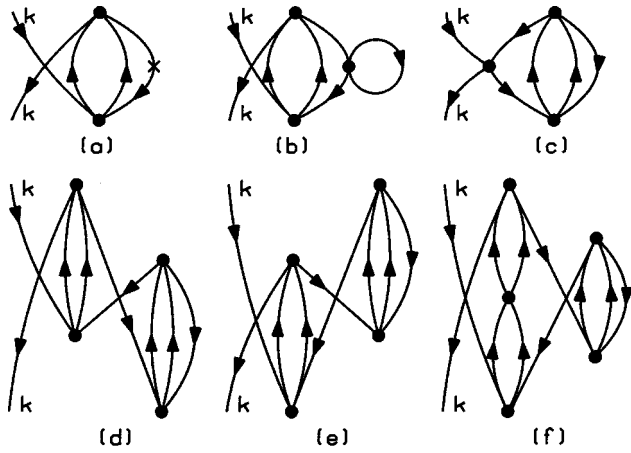
FIG. 14. First members of the infinite series of diagrams which can be built by assembling (2, 1) subdiagrams with (4, 0) subdiagrams.

bined with both the $n=0$ and $n=1$ versions of the subdiagram in Fig. 13(b). This yields the diagrams depicted in Figs. 14(d), 14(e), and 14(f). One checks that, in general, G-matrix ladders in the complete diagrams will be avoided only by combining the n version of the subdiagram in Fig. 12(c) with the $n-1$, n, or $n+1$ versions of the subdiagram in Fig. 13(b). Using the Bethe-Brandow-Petscheck (BBP) theorem [6], one sees that the whole series of $(2, 1)+(4, 0)$ diagrams without U insertions boils down to the two diagrams depicted in Fig. 15 where the label ''on'' means that the G matrices in the middle of the diagrams should be calculated on the energy shell. The diagram 15(a) is cancelled by the diagram 14(a) when the auxiliary potential for hole states is chosen self-consistently at the one hole line level, i.e., is identified by the BHF contribution to the mass operator [see Fig. 9(a)]. The diagram 15(b) renormalizes the BHF contribution [7].

To complete the example, let us consider the diagrams resulting from the assembly of two (4, 0) subdiagrams. The diagram in Fig. 13(a) can only be assembled with the $n=0$ version of the diagram in Fig. 13(b). This yields the diagrams depicted in Figs. 16(a) and 16(b). The n version of the subdiagram 13(b) can be combined with both the n and the $n+1$ version of the same subdiagram. The diagrams corresponding to $n=0$ are depicted in Figs. 16(c)–16(f). Again the BBP theorem can be used to reduce the whole series of $(4, 0)+(4, 0)$ diagrams to the two diagrams of Fig. 17, where the middle G matrix has to be calculated on the energy shell.

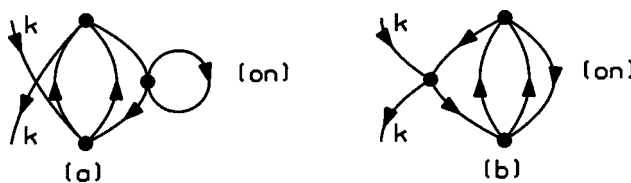Note finally that all the mass operator diagrams composed of two subdiagrams (see Figs. 14–17) can be obtained from
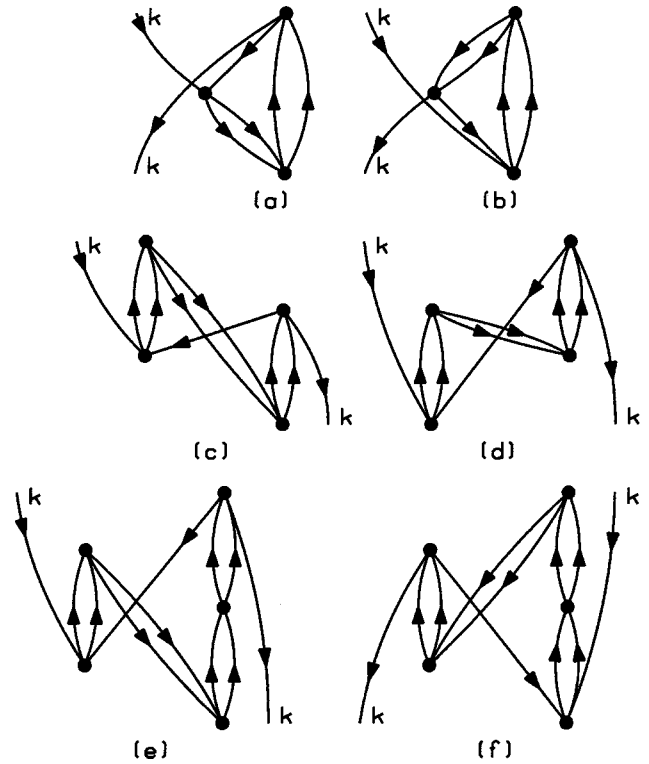

FIG. 16. First members of the infinite series of diagrams which can be built by assembling two (4, 0) subdiagrams.

corresponding binding energy diagrams. For instance, by cutting a hole line in the hole-hole diagram of Fig. 1, one accounts for the two diagrams of Fig. 17.

V. SUMMARY AND DISCUSSION

In this paper, we have discussed the enumeration problems appearing within the hole line expansion method. The diagrams contributing to a given order I cannot be obtained by the straightforward enumeration of the diagrams with I hole lines. What matters is the number of independent hole lines, i.e., the number of hole lines whose momenta are not fixed by momentum conservation. From a practical point of view, this immediately leads us to inquire whether there is an upper bound on the number h of hole lines which can appear in the diagrams contributing to a given order I. Here, we have discussed the binding energy and mass operator cases for which we have found the upper bounds given by Eqs. (2.5) and (2.11), respectively. We have also shown that it is not necessary to enumerate all the diagrams within these up-
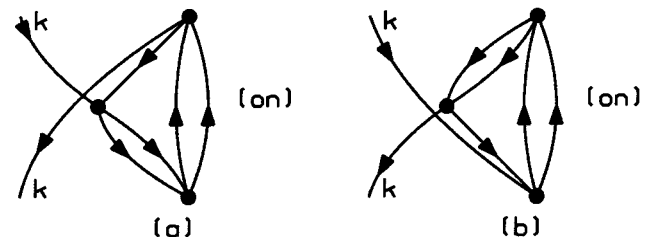

FIG. 15. Diagrams resulting from the BBP summation of the whole series of $(2, 1)+(4, 0)$ diagrams without U insertions. The labels ''on'' mean that the middle G matrices should be calculated on the energy shell.

FIG. 17. Diagrams resulting from the BBP summation of the whole series of $(4, 0)+(4, 0)$ diagrams. The labels ''on'' mean that the middle G matrices should be calculated on the energy shell.

per bounds. Indeed, we have proved that the diagrams with $h > I$ can be constructed from a well defined number of sub-diagrams whose enumeration is much easier than that of the diagrams they are composing. As far as we know, the enumeration problems posed by the hole line expansion were considered systematically only in [2] and [8]. Reference [2] was concerned with the enumeration of the $I = 4$ contributions to the binding energy of nuclear matter. Actually, the method which was used to arrive at the full set of these diagrams was not described at all. We can check, however, that all these diagrams have at most six hole lines, i.e., satisfy in the $I = 4$ case the upper bound given in general by Eq. (2.5). Let us also emphasize that the combination diagrams of [2], which are defined at a given order I of the hole line expansion as the diagrams whose energy denominators, possibly after applying the BBP theorem, do not involve the excitation of I particles above the Fermi surface, should not be identified with the diagrams composed of subdiagrams which have been considered in the present paper. An example of a combination diagram which is not composed of subdiagrams is given in Fig. 18. On the other hand, all diagrams composed of subdiagrams are combination diagrams. This statement can be proved by noting that it is logically equivalent to the statement that diagrams which are not combination diagrams cannot be disconnected by suppressing their hole lines. The latter statement is obvious because the diagrams which are not combination diagrams at the order I of the hole line expansion coincide with the so-called I-body cluster diagrams, i.e., with the diagrams which, after suppression of their hole lines, appear as I upgoing lines connected by a certain number of antisymmetrized G matrices. As with [2], [8] is also concerned with the binding en-
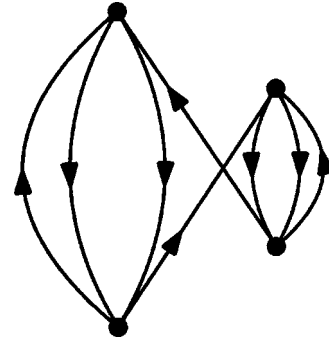

FIG. 18. Example of diagram which would be considered as a combination diagram according to [2] although it consists of a single subdiagram.

ergy of nuclear matter but the enumeration of diagrams is considered at any order I of the hole line expansion. It was also found that the enumeration work is ''bounded'' by an inequality which has to be satisfied at any given order I (see Eq. (34) of [8]). Note, however, that the method used in [8] is an algebraic one and as a consequence this inequality is different from our inequality Eq. (2.5): it refers more to the algebraic expression of the binding energy (see Eq. (30) of [8]) than to the structure of the diagrams. This leads to some extra work of elimination of unwanted diagrams (see point (ii) in the rule summary of [8]) which is avoided here by taking into account the structure in subdiagrams. Finally, note that the quantity denoted by C in [8], i.e., the number of momentum conservation conditions for hole lines which apply in a diagram, can actually be determined readily by means of the tree analysis we described in Sec. II.

---

[1] *Nuclear Methods and the Nuclear Equation of State*, edited by M. Baldo (World Scientific, Singapore, in press).
[2] B. D. Day, Phys. Rev. **187**, 1269 (1969).
[3] J. Hüfner and C. Mahaux, Ann. Phys. (N.Y.) **73**, 525 (1972).
[4] B. D. Day, Phys. Rev. C **24**, 1203 (1981).
[5] C. Mahaux and R. Sartor, Phys. Rev. C **19**, 229 (1979).
[6] H. A. Bethe, B. H. Brandow, and A. G. Petscheck, Phys. Rev. **129**, 225 (1963).
[7] M. Baldo, I. Bombaci, G. Giansiracusa, U. Lombardo, C. Mahaux, and R. Sartor, Phys. Rev. C **41**, 1748 (1990), and references therein.
[8] T. H. Schucan and H. A. Weidenmüller, Phys. Rev. C **3**, 1856 (1971).